VIP Phosphorylation Very Important Paper

Deutsche Ausgabe: DOI: 10.1002/ange.201603797
Internationale Ausgabe: DOI: 10.1002/anie.201603797

Discovery of a Highly Selective Glycogen Synthase Kinase-3 Inhibitor (PF-04802367) That Modulates Tau Phosphorylation in the Brain: Translation for PET Neuroimaging

Steven H. Liang[+], Jinshan Michael Chen[+], Marc D. Normandin, Jeanne S. Chang, George C. Chang, Christine K. Taylor, Patrick Trapa, Mark S. Plummer, Kimberly S. Para, Edward L. Conn, Lori Lopresti-Morrow, Lorraine F. Lanyon, James M. Cook, Karl E. G. Richter, Charlie E. Nolan, Joel B. Schachter, Fouad Janat, Ye Che, Veerabahu Shanmugasundaram, Bruce A. Lefker, Bradley E. Enerson, Elijahu Livni, Lu Wang, Nicolas J. Guehl, Debasis Patnaik, Florence F. Wagner, Roy Perlis, Edward B. Holson, Stephen J. Haggarty, Georges El Fakhri, Ravi G. Kurumbail, and Neil Vasdev**

Abstract: *Glycogen synthase kinase-3 (GSK-3) regulates multiple cellular processes in diabetes, oncology, and neurology. N-(3-(1H-1,2,4-triazol-1-yl)propyl)-5-(3-chloro-4-methoxyphenyl)oxazole-4-carboxamide (PF-04802367 or PF-367) has been identified as a highly potent inhibitor, which is among the most selective antagonists of GSK-3 to date. Its efficacy was demonstrated in modulation of tau phosphorylation in vitro and in vivo. Whereas the kinetics of PF-367 binding in brain tissues are too fast for an effective therapeutic agent, the pharmacokinetic profile of PF-367 is ideal for discovery of radiopharmaceuticals for GSK-3 in the central nervous system. A ^{11}C-isotopologue of PF-367 was synthesized and preliminary PET imaging studies in non-human primates confirmed that we have overcome the two major obstacles for imaging GSK-3, namely, reasonable brain permeability and displaceable binding.*

Glycogen synthase kinase 3 (GSK-3) is a serine and threonine kinase that regulates a plethora of physiological functions in the periphery and central nervous system (CNS), ranging from differentiation and development, to metabolism, cell cycle regulation, and neuroprotection.[1] GSK-3 plays a significant role in several pathologies, including Alzheimer's disease (AD), mood disorders, type-II diabetes, and in some cancers.[2] Specifically for neurodegenerative diseases, molecular imaging of GSK-3 can indicate target engagement by GSK-3 therapeutics and offer a path to diagnostic agents that not only correlates with early cognitive impairment, but also increased tau hyperphosphorylation,[2a,3] increased amyloid-production,[4] and local plaque-associated glial-mediated inflammatory responses; all of which are hallmarks of AD and non-AD tauopathies. GSK-3 plays a key role in AD, evident from: 1) the abundance and dysregulation of GSK-3 in the AD brain;[5] 2) reduced tau phosphorylation (P-tau) induced by treatment with GSK-3β inhibitors;[6] and 3) genetic studies suggesting GSK-3 is fundamental in the pathogenesis of sporadic and familial AD. These and related findings have led to the GSK-3 hypothesis of Alzheimer's disease.[7]

The pertinence of GSK-3 in diverse diseases has led to long-standing efforts to develop small-molecule inhibitor-based therapeutics.[8] Clinical translation of potent GSK-3 therapeutics for neurodegenerative disease have faced three major hurdles: 1) poor GSK-3 selectivity over other CNS targets and closely related kinases; 2) low blood–brain barrier (BBB) penetration; and 3) chronic toxicity. A positron emission tomography (PET) radiotracer for GSK-3 could aid many ongoing clinical research efforts to develop GSK-3 targeted therapeutics by indicating the success and extent of engagement by GSK-3 inhibitors in the brain. However, the

[*] Prof. Dr. S. H. Liang,[+] Prof. Dr. M. D. Normandin, Prof. Dr. E. Livni, L. Wang, Dr. N. J. Guehl, Prof. Dr. G. El Fakhri, Prof. Dr. N. Vasdev
Gordon Center for Medical Imaging & Nuclear Medicine and Molecular Imaging
Massachusetts General Hospital & Department of Radiology
Harvard Medical School, Boston, MA 02114 (USA)
E-mail: vasdev.neil@mgh.harvard.edu

Dr. J. M. Chen,[+] Dr. J. S. Chang, Dr. G. C. Chang, Dr. C. K. Taylor, Dr. M. S. Plummer, Dr. K. S. Para, Dr. E. L. Conn, Dr. L. Lopresti-Morrow, Dr. L. F. Lanyon, Dr. J. M. Cook, Dr. K. E. G. Richter, Dr. C. E. Nolan, Dr. J. B. Schachter, Dr. F. Janat, Dr. Y. Che, Dr. V. Shanmugasundaram, Dr. B. E. Enerson, Dr. R. G. Kurumbail
Pfizer Worldwide Research and Development, Groton Laboratories
Eastern Point Road, Groton, CT 06340 (USA)
E-mail: ravi.g.kurumbail@pfizer.com

Dr. P. Trapa, Dr. B. A. Lefker
Pfizer Worldwide Research and Development
610 Main Street, Cambridge, MA 02139 (USA)

F. F. Wagner, Prof. Dr. R. Perlis, Dr. E. B. Holson
Stanley Center for Psychiatric Research, Broad Institute
415 Main Street, Cambridge, MA o2142 (USA)

Dr. D. Patnaik, Prof. Dr. R. Perlis, Prof. Dr. S. J. Haggarty
Departments of Neurology & Psychiatry
Massachusetts General Hospital, Harvard Medical School
185 Cambridge Street, Boston, MA 02114 (USA)

[+] These authors contributed equally to this work.

Supporting information for this article can be found under: http://dx.doi.org/10.1002/anie.201603797.

greatest obstacles for molecular neuroimaging of GSK-3 has been with the discovery of potent and highly selective small molecules with reasonable brain penetration. Our initial work to develop a PET radiotracer for GSK-3[9] focused on ^{11}C-labeled isotopologues of AR-A014418,[9a,10] and other scaffolds were subsequently explored. Only three other radiotracers for GSK-3 have been studied in vivo. [^{11}C]SB-216763 showed good brain uptake in rodents and non-human primates (NHPs) but was not selective against other structurally similar kinases.[11] [^{11}C]PyrATP-1[12] and ^{11}C-oxadiazole[13]-based radiotracers failed to show appreciable uptake in vivo. None of the PET radiotracers for GSK-3 has yet proven to be successful for in vivo imaging studies with specificity and/or suitable brain uptake (Figure 1). Thus an

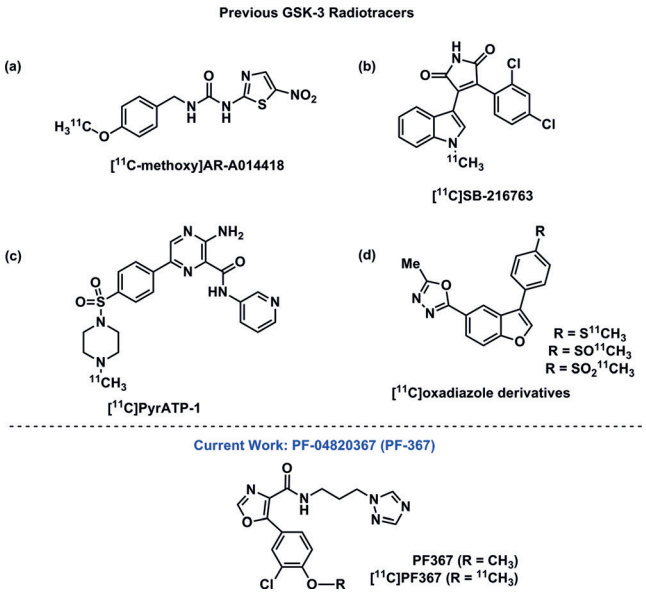

Figure 1. Previous attempts for the development of GSK-3 PET ligands, and this work. PF-04802367 is commercially available from Sigma Aldrich (catalogue no. PZ0313).

acute need for PET neuroimaging of GSK-3 remains, specifically for clinical research applications in AD and non-AD tauopathies.[14] We report herein a potent GSK-3 inhibitor [*N*-(3-(1*H*-1,2,4-triazol-1-yl)propyl)-5-(3-chloro-4-methoxyphenyl)oxazole-4-carboxamide; PF-04802367 or PF-367) with exceptional kinome selectivity that modulates phosphorylated tau levels in vivo. Preliminary PET imaging studies using carbon-11 (^{11}C; β^+, $t_{1/2} = 20.4$ min) labeled PF-367 (Figure 1) in NHPs unveils this radiotracer as a promising diagnostic imaging agent for GSK-3 levels in the living brain.

A small molecule inhibitor of GSK-3 was identified from a high-throughput screening hit using structure-based drug design (PF-856; Supporting Information, Figure S1). Multiparameter optimization (MPO)[15] of physical properties for computational predictions of BBB penetration was used to optimize PF-856 and led us to PF-367, a 4-carboxamide 5-aryl disubstituted oxazole bearing a triazole at the terminal side chain. PF-367 has a half-maximal inhibitory concentration (IC_{50}) of 2.1 nM based on a recombinant human GSK-3β

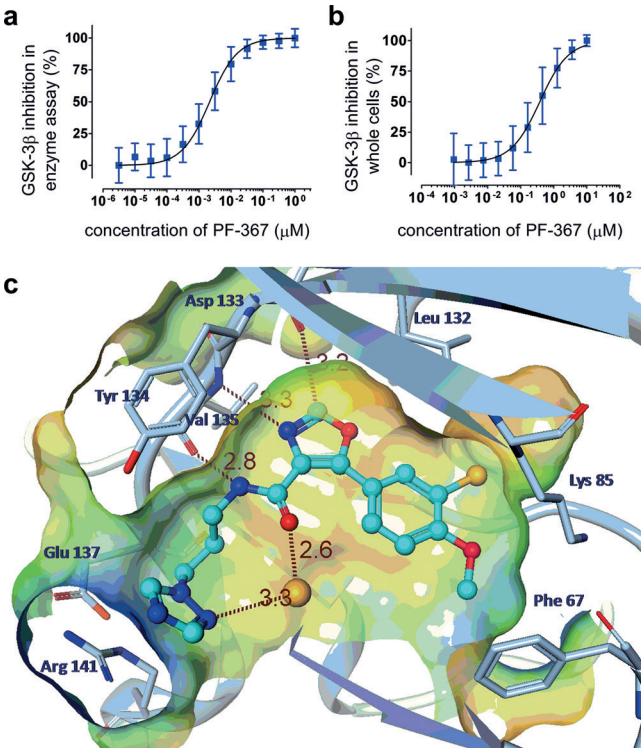

Figure 2. In vitro screening and crystallographic structure to identify PF-367 as a potent GSK-3β inhibitor.

enzyme assay (Figure 2a) and 1.1 nM based on ADP-Glo assay, and a favorable MPO score of 5.65 (out of maximal score of 6.0). In mobility shift assays, PF-367 was equally effective at inhibition of the two known GSK-3 isoforms (GSK-3α and GSK-3β) with IC_{50} values of 10.0 and 9.0 nM, respectively. PF-367 was efficient at inhibiting GSK-3β enzymatic activity in vitro with ligand and lipophilic efficiency scores of 0.46 and 7.0, respectively. Moreover, PF-367 has reasonable in vitro stability in human hepatic microsomes ($t_{1/2} = 78.7$ min), has excellent passive permeability, as measured in an MDCK MDR cell line ($> 20 \times 10^{-6}$ cm s^{-1}). Fortunately PF-367 is not a candidate for efflux by P-glycoprotein as measured in the MDCK MDR cell line (BA/AB = 1.26). In a stable inducible CHO cell line overexpressing GSK-3β and its substrate tau, PF-367 inhibited phosphorylation of tau with an IC_{50} of 466 nM (Figure 2b). Preclinical safety evaluations showed that PF-367 has good cell viability (IC_{50} of 117 μM in THLE cytotoxicity assays) and an $IC_{50} > 100$ μM in a hERG screening assay. Furthermore, PF-367 was negative in gene toxicity assays (in vitro micronucleus assay and Ames test) and in broad ligand profiling against a diverse panel of proteins. Thus, PF-367 demonstrated exceptional potency, permeability, stability and safety profile as a novel GSK-3 inhibitor in vitro.

X-ray crystallographic studies were conducted to explore the molecular mechanism responsible for the high potency of PF-367. A 2.2 Å co-crystal structure of PF-367 bound to GSK-3β showed that it is a typical Type I kinase inhibitor that binds at the ATP site of kinases between the *N*- and *C*-lobes (Figure 2c; PDB code: 5K5N). The oxazole and amide nitrogen atoms of PF-367 form donor–acceptor hydrogen

bonds with Val 135 at the ATP site. Furthermore, the carbon at the 2-position of the oxazole ring forms a non-classical hydrogen bond with the carbonyl oxygen of Asp 133. The phenyl ring is co-planar with the oxazole ring and is sandwiched between residues from the P-loop and C-lobe of the kinase. The chlorine at the 3-position of the phenyl ring displaces a bound water molecule which could account for the increased potency observed in analogues that contain a halogen or methyl group at this position. The 4-methoxy substituent abuts the conserved lysine (Lys 85) and Phe 67 from the P-loop. The propyl linker connecting the amide and the terminal triazole ring positions the latter near the solvent front and in a suitable geometry and distance to form strong cation-π interaction with Arg 141 from the kinase hinge peptide. Moreover, the side-chain guanidinium group of Arg 141 is held in a rigid position by an ion-pair with the carboxylate of Glu 137 (Supporting Information, Figure S2).

To evaluate the kinome selectivity, PF-367 was screened against a broad panel of 240 kinases in biochemical functional assays at a concentration of 10 μM. Only 6 kinases (including GSK-3α/β) out of 240 showed more than 65% inhibition at this concentration (Supporting Information, Figure S3). We further profiled PF-367 against a more comprehensive DiscoverRx kinome panel of 386 unique kinases (442 total) that relies on competitive displacement of known probes from kinase ATP site (ca. 75% of the kinome). In this panel, PF-367 crossed over to only 18 kinases (including GSK-3α/β) with more than 65% inhibition (Supporting Information, Figure S4). Gaining selectivity over cyclin-dependent kinase 2 (CDK2) has been a challenge for most GSK-3 inhibitors owing to the similarities in the ATP sites of these two kinases. In this pan-kinase selectivity screening assay, we observed that PF-367 was greater than 1000-fold selective for GSK-3α/β over CDK2. Concentration–activity relationship studies against this small subset of interacting kinases showed that PF-367 exhibited greater than 450-fold selectivity for GSK-3α/β over all kinases tested and is one of the most selective ATP-competitive kinase inhibitors reported (Figure 3). Inhibition of GSK-3 could lead to activation of the canonical Wnt signaling pathway, which results in accumulation of β-catenin in cytoplasm and its subsequent translocation to the nucleus, triggering gene transcription events and cell proliferation by association with the T-cell factor/lymphoid enhancing factor.[16] To assess this potential risk factor, we evaluated PF-367 in a number of cellular assays downstream of Wnt/β-catenin signaling, including nuclear translocation of β-catenin, gene transcription (TOPFlash luciferase reporter assay) and proliferation (incorporation of Ki-67) assays. Relative to its cellular potency in modulating phospho-Tau levels, PF-367 showed significant right shifts against β-catenin translocation in HeLa cells with EC_{50} of 6.2 μM, gene transcription in U20S cells with EC_{50} of 20.6 μM, and cell proliferation in HeLa cells as evaluated by Ki-67 incorporation with EC_{50} of 9.0 μM (Supporting Information, Figure S5).

The promising in vitro profile and ADME properties suggests that PF-367 could modulate phosphorylation of tau protein (P-tau) in vivo through inhibition of GSK-3. Using specific antibodies directed toward phospho-Tau epitopes (AT8 and PHF-13), we evaluated the pharmacodynamic effects of PF-367 in rodent models. A single dose (50 mg kg^{-1}, subcutaneous) of PF-367 showed a rapid 76% reduction of P-tau levels in the brain and 92% reduction of phosphoglycogen synthase (pGS) in skeletal muscle after one hour of administration in rats (Figure 4a). Moreover, dose-dependent

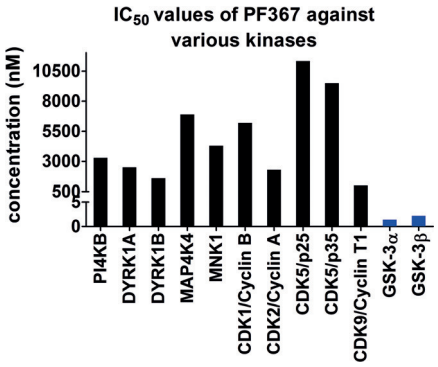

Figure 3. Biochemical inhibition of selected kinases by PF-367 showing selective modulation of GSK-3 in kinome pathway. PF-367 selectively binds GSK-3α/3β among all 240 kinase tested. Kinase activities are given as the mean of triplicate experiments.

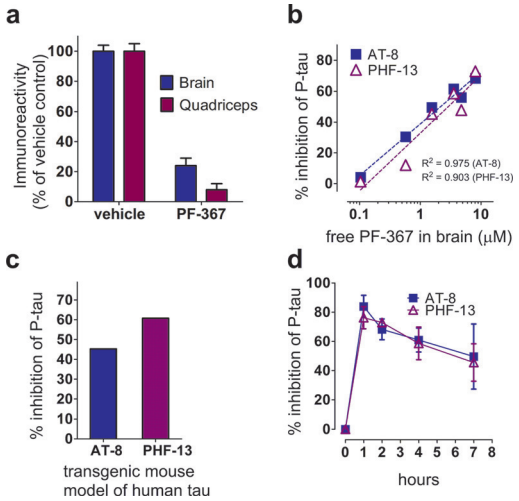

Figure 4. In vivo efficacy of PF-367 in Sprague–Dawley rats and transgenic model of human tau mice. a) Inhibition of tau phosphorylation in both CNS and the periphery. b) Free fraction of PF-367 in brain correlates directly with % inhibition of P-tau in the brain. c) Inhibition of tau phosphorylation in transgenic model of human tau mice (Tg4510). d) PF-367 delivered orally inhibits phosphorylation of tau in brain.

inhibition of P-tau by PF-367 was observed in the rat brain with maximal inhibition of about 50% in P-tau levels at 50 mg kg^{-1} with a free drug exposure of about 5 μM in the brain (Supporting Information, Figure S6). We observed a direct linear correlation between unbound drug fractions of PF-367 and % inhibition of P-tau in rat brain, suggesting a linear PK-PD relationship (Figure 4b). The effect of PF-367 on P-tau was also validated in a transgenic mouse model (Tg4510) of human tauopathy (Figure 4c), which showed similar effect in modulating P-tau levels. Oral administration

of PF-367 in rats showed up to 83% inhibition of P-tau after one hour with at least 50% reduction even after seven hours (Figure 4d). The pharmacokinetic response was slightly delayed with respect to the pharmacodynamic effect of P-tau modulation, with free brain drug exposures of 8 μM at 2 hours which progressively decreased to 2 μM after seven hours (Supporting Information, Figure S7). These data suggest that PF-367 is effective at inhibiting tau phosphorylation in rodent models, and is consistent with our observations of GSK-3 inhibition in biochemical and whole cell assays.

Despite overcoming several hurdles for discovery of a therapeutic for GSK-3, the short in vivo half-life of PF-367 precluded any long-term chronic behavioral studies and kinetics of PF-367 binding in brain tissues are too fast for an effective therapeutic agent. However, the pharmacokinetic profile of PF-367 is ideal for discovery of radiotracers that target GSK-3 in the CNS. [^{11}C]PF-367 was synthesized in ca. 5% uncorrected radiochemical yield (relative to [^{11}C]CO_2) by reaction of the corresponding phenolic precursor in the presence of base with [^{11}C]CH_3I with specific activity >2 Ci μmol^{-1} (Figures 5a; Supporting Information, Figures S8, S9). Two rhesus macaques each underwent two PET scans. The first was a baseline scan in which high specific activity [^{11}C]PF-367 was administered and the second was a blocking scan that included [^{11}C]PF-367 plus 135 μg kg^{-1} of unlabeled PF-367. Dynamic PET scans were acquired for 120 minutes and included arterial sampling with radiometabolite correction for estimation of the [^{11}C]PF-367 arterial input function. [^{11}C]PF-367 ($\log D_{7.4} = 2.14$) showed good brain penetration (1 SUV; standardized uptake value) with similar uptake immediately after radiotracer injection in baseline and blocking experiments. As predicted, blocking experiments showed a more rapid clearance of [^{11}C]PF-367 owing to reduced availability of binding sites and resulted in lower brain concentrations at later times (Figure 5b–d; Supporting Information, Figures S10, S11). Kinetic analyses indicate regional reductions in displaceable specific binding of approximately 30%. These initial imaging studies confirm that [^{11}C]PF-367 readily crosses the BBB and has favorable characteristics warranting further evaluation as a PET tracer for in vivo quantification of GSK-3 expression. Our future work includes further PET imaging, including occupancy studies, in NHPs and post-mortem analysis in GSK-3 rodent models.

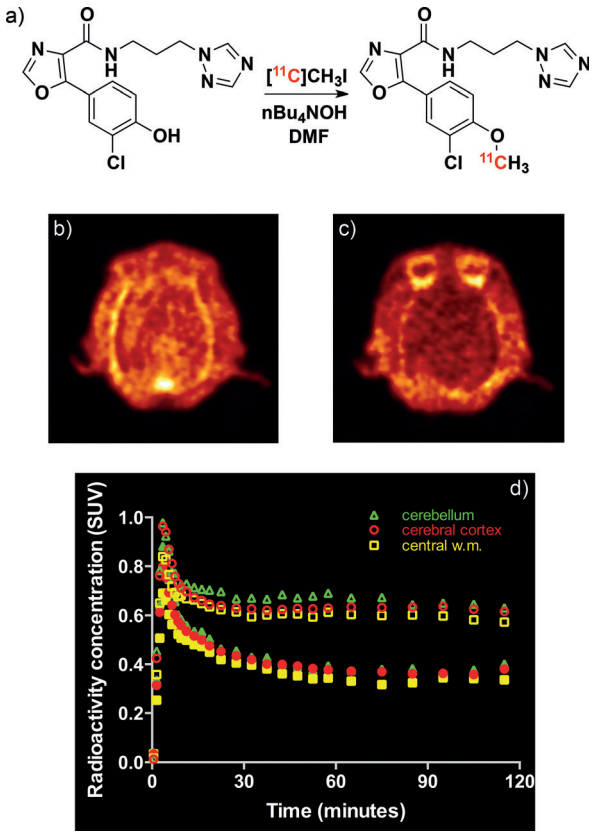

Figure 5. a) [^{11}C]PF-367 visualizes GSK-3 distribution in the living brain. b),c) Representative summed PET images (30–60 min) for baseline and blocking studies, respectively. d) Regional time activity curves (cerebellum, cerebral cortex and central white matter) extracted from the baseline (open symbols) and blocking (filled symbols) PET studies.

In summary, PF-367 was discovered to be a highly potent and selective inhibitor of GSK-3, with efficacy in modulation of tau phosphorylation in vitro and in vivo, and it displays excellent bioavailability. Based on functional and competitive binding assays against a wide panel of protein kinases, we have shown that PF-367 represents one of the most selective inhibitors of GSK-3 reported to date. X-ray crystal-structure analysis and structure activity relationships suggest that PF-367 attains its potency and selectivity by forming strong cation-π interactions with a relatively rigid arginine at the ATP site of GSK-3β. Preliminary PET imaging studies with [^{11}C]PF-367 confirmed reasonable brain permeability and specificity in the non-human primate brain, making it an outstanding lead neuroimaging agent for GSK-3.

Acknowledgements

We thank Rebecca Lewis, Justin Pine, Patricia Cosgrove, Jeffrey Asbill, Dr. Dustin Wooten, Dr. T. Lee Collier, and Dr. Lee Josephson for technical support and helpful discussions. We thank Seungil Han, Mark Ammirati, Mathew Calabrese, Jayvardhan Pandit, and Mathew Griffor for crystallographic studies, supported by Hauptman-Woodward Medical Research Institute and IMCA-CAT at Advanced Photon Source, U.S. Department of Energy (DE-AC02-06CH11357). S.H.L. is a recipient of an NIH career development award (NIDA 1K01DA038000). S.J.H. was supported in part by the Tau Consortium.

Keywords: Alzheimer's disease · glycogen synthase kinase-3 · phosphorylation · positron emission tomography · tau proteins

How to cite: *Angew. Chem. Int. Ed.* **2016**, *55*, 9601–9605
Angew. Chem. **2016**, *128*, 9753–9757

[1] a) J. R. Woodgett, *EMBO J.* **1990**, *9*, 2431–2438; b) J. R. Woodgett, in *Glycogen Synthase Kinase 3 (GSK-3) and Its Inhibitors: Drug Discovery and Development*, Wiley, Hoboken, **2006**, pp. 3–23; c) R. S. Jope, G. V. W. Johnson, *Trends Biochem. Sci.* **2004**,

29, 95 – 102; d) L. Meijer, M. Flajolet, P. Greengard, *Trends Pharmacol. Sci.* **2004**, *25*, 471 – 480; e) P. Lei, S. Ayton, A. I. Bush, P. A. Adlard, *Int. J. Alzheimers Dis.* **2011**, 9; f) C. A. Thorne, C. Wichaidit, A. D. Coster, B. A. Posner, L. F. Wu, S. J. Altschuler, *Nat. Chem. Biol.* **2015**, *11*, 58 – 63.

[2] a) A. Martinez, D. I. Perez, C. Gil, *Curr. Top. Med. Chem.* **2013**, *13*, 1808 – 1819; b) M. K. Pandey, T. R. DeGrado, *Theranostics* **2016**, *6*, 571 – 593.

[3] a) M. Takahashi, K. Tomizawa, R. Kato, K. Sato, T. Uchida, S. C. Fujita, K. Imahori, *J. Neurochem.* **1994**, *63*, 245 – 255; b) Y. Wang, E. Mandelkow, *Nat. Rev. Neurosci.* **2016**, *17*, 22 – 35.

[4] B. DaRocha-Souto, M. Coma, B. G. Perez-Nievas, T. C. Scotton, M. Siao, P. Sanchez-Ferrer, T. Hashimoto, Z. Fan, E. Hudry, I. Barroeta, L. Sereno, M. Rodriguez, M. B. Sanchez, B. T. Hyman, T. Gomez-Isla, *Neurobiol. Dis.* **2012**, *45*, 425 – 437.

[5] a) J. J. Lucas, F. Hernandez, P. Gomez-Ramos, M. A. Moran, R. Hen, J. Avila, *EMBO J.* **2001**, *20*, 27 – 39; b) F. Hernandez, J. Borrell, C. Guaza, J. Avila, J. J. Lucas, *J. Neurochem.* **2002**, *83*, 1529 – 1533; c) A. Fuster-Matanzo, M. Llorens-Martín, E. G. de Barreda, J. Ávila, F. Hernández, *PLoS ONE* **2011**, *6*, e27262; d) M. Sirerol-Piquer, P. Gomez-Ramos, F. Hernández, M. Perez, M. A. Morán, A. Fuster-Matanzo, J. J. Lucas, J. Avila, J. M. García-Verdugo, *Hippocampus* **2011**, *21*, 910 – 922; e) K. Leroy, Z. Yilmaz, J. P. Brion, *Neuropathol. Appl. Neurobiol.* **2007**, *33*, 43 – 55.

[6] D. E. Hurtado, L. Molina-Porcel, J. C. Carroll, C. Macdonald, A. K. Aboagye, J. Q. Trojanowski, V. M. Lee, *J. Neurosci.* **2012**, *32*, 7392 – 7402.

[7] C. Hooper, R. Killick, S. Lovestone, *J. Neurochem.* **2008**, *104*, 1433 – 1439.

[8] a) P. Cohen, M. Goedert, *Nat. Rev. Drug Discovery* **2004**, *3*, 479 – 487; b) G. Luo, L. Chen, C. R. Burton, H. Xiao, P. Sivaprakasam, C. M. Krause, Y. Cao, N. Liu, J. Lippy, W. J. Clarke, K. Snow, J. Raybon, V. Arora, M. Pokross, K. Kish, H. A. Lewis, D. R. Langley, J. E. Macor, G. M. Dubowchik, *J. Med. Chem.* **2016**, *59*, 1041 – 1051; c) G. Gentile, G. Merlo, A. Pozzan, G. Bernasconi, P. Bamborough, A. Bridges, P. Carter, M. Neu, G. Yao, C. Brough, G. Cutler, A. Coffin, S. Belyanskaya, *Bioorg. Med. Chem. Lett.* **2012**, *22*, 1989 – 1994; d) S. Berg, M. Bergh, S. Hellberg, K. Högdin, Y. Lo-Alfredsson, P. Söderman, S. von Berg, T. Weigelt, M. Ormö, Y. Xue, J. Tucker, J. Neelissen, E. Jerning, Y. Nilsson, R. Bhat, *J. Med. Chem.* **2011**, *54*, 9107 – 9119.

[9] a) N. Vasdev, A. Garcia, W. T. Stableford, A. B. Young, J. H. Meyer, S. Houle, A. A. Wilson, *Bioorg. Med. Chem. Lett.* **2005**, *15*, 5270 – 5273; b) J. W. Hicks, H. F. VanBrocklin, A. A. Wilson, S. Houle, N. Vasdev, *Molecules* **2010**, *15*, 8260 – 8278.

[10] J. W. Hicks, A. A. Wilson, E. A. Rubie, J. R. Woodgett, S. Houle, N. Vasdev, *Bioorg. Med. Chem. Lett.* **2012**, *22*, 2099 – 2101.

[11] a) M. Wang, M. Gao, K. D. Miller, G. W. Sledge, G. D. Hutchins, Q.-H. Zheng, *Bioorg. Med. Chem. Lett.* **2011**, *21*, 245 – 249; b) L. Li, X. Shao, E. L. Cole, S. A. Ohnmacht, V. Ferrari, Y. T. Hong, D. J. Williamson, T. D. Fryer, C. A. Quesada, P. Sherman, P. J. Riss, P. J. H. Scott, F. I. Aigbirhio, *ACS Med. Chem. Lett.* **2015**, *6*, 548 – 552.

[12] E. L. Cole, X. Shao, P. Sherman, C. Quesada, M. V. Fawaz, T. J. Desmond, P. J. H. Scott, *Nucl. Med. Biol.* **2014**, *41*, 507 – 512.

[13] K. Kumata, J. Yui, L. Xie, Y. Zhang, N. Nengaki, M. Fujinaga, T. Yamasaki, Y. Shimoda, M.-R. Zhang, *Bioorg. Med. Chem. Lett.* **2015**, *25*, 3230 – 3233.

[14] J. P. Holland, S. H. Liang, B. H. Rotstein, T. L. Collier, N. A. Stephenson, I. Greguric, N. Vasdev, *J. Labelled Compd. Radiopharm.* **2014**, *57*, 323 – 331.

[15] T. T. Wager, X. Hou, P. R. Verhoest, A. Villalobos, *ACS Chem. Neurosci.* **2010**, *1*, 435 – 449.

[16] J. V. Wauwe, B. Haefner, *Drug News Perspect.* **2003**, *16*, 557 – 565.

Received: April 19, 2016
Published online: June 29, 2016

